

## Supporting Information for

### ***In vivo* activation of the p53 tumor suppressor pathway by an engineered cyclotide**

Yanbin Ji<sup>a,1</sup>, Subhabrata Majumder<sup>c,1</sup>, Melissa Millard<sup>a,1</sup>, Radhika Borra<sup>a,1</sup>, Tao Bi<sup>a,1</sup>, Ahmed Y. Elnagar<sup>a,1</sup>, Nouri Neamati<sup>a</sup>, Alexander Shekhtman<sup>c</sup> and Julio A. Camarero<sup>a,b,2</sup>

<sup>a</sup>*Department of Pharmacology and Pharmaceutical Sciences and* <sup>b</sup>*Department of Chemistry, University of Southern California, Los Angeles, CA 90033, USA;* <sup>c</sup>*Department of Chemistry, State University of New York, Albany, NY 12222, USA*

**Materials and instrumentation.** Analytical HPLC was performed on a HP1100 series instrument with 220 nm and 280 nm detection using a Vydac C18 column (5  $\mu$ m, 4.6 x 150 mm) at a flow rate of 1 mL/min. Semipreparative HPLC was performed on a Waters Delta Prep system fitted with a Waters 2487 Ultraviolet-Visible (UV-vis) detector using a Vydac C18 column (15-20  $\mu$ m, 10 x 250 mm) at a flow rate of 5 mL/min. All runs used linear gradients of 0.1% aqueous trifluoroacetic acid (TFA, solvent A) vs. 0.1% TFA, 90% acetonitrile in H<sub>2</sub>O (solvent B). UV-vis spectroscopy was carried out on an Agilent 8453 diode array spectrophotometer, and fluorescence analysis on a Flurolog-3 spectrofluorimeter (Horiba Scientific). Electrospray mass spectrometry (ES-MS) analysis was routinely applied to all cyclized peptides. ES-MS was performed on an Applied Biosystems API 3000 triple quadrupole electrospray mass spectrometer using Analyst 1.4.2. LC-MS was performed on a HP1100 HPLC/API-3000 system using a multiple reaction monitoring (MRM) mode. Calculated masses were obtained by using ProMac v1.5.3. Protein samples were analyzed by SDS-PAGE. Samples were run on Invitrogen (Carlsbad) 4-20% Tris-Glycine Gels. The gels were then stained with Pierce (Rockford) Gelcode Blue, photographed/digitized using a Kodak (Rochester) EDAS 290, and quantified using NIH Image-J software (<http://rsb.info.nih.gov/ij/>). DNA sequencing was performed by the DNA Sequencing and Genetic Analysis Core Facility at the University of Southern California using an ABI 3730 DNA sequencer, and the sequence data was analyzed with DNASTar Lasergene v5.5.2. All chemicals were obtained from Sigma-Aldrich unless otherwise indicated. Nutlin-3 was purchased from sellechchem.com ([www.sellechchem.com](http://www.sellechchem.com)).

**Preparation of Fmoc-Tyr(tBu)-F.** Fmoc-Tyr(tBu)-F was prepared using diethylaminosulfur trifluoride (DAST) [1] and quickly used afterwards. To a stirred solution of the Fmoc-amino acid (10 mmol) in 60 mL of dry dichloromethane (DCM), under an argon atmosphere, 805  $\mu$ L (10 mmol) of pyridine (dry) were added at room temperature followed by dropwise addition of 1.57

mL (12 mmol) of DAST. After stirring for 20 min, the mixture was extracted three times with 150 mL of ice water and the combined organic layers were dried over  $\text{MgSO}_4$  and molecular sieves (10 Å). The solvent was removed *in vacuo* at room temperature. Recrystallization or precipitation from DCM/n-hexane gave the Fmoc-amino acid fluoride.

**Loading of 4-sulfamylbutyryl AM resin with Fmoc-Tyr(tBu)-F.** Loading of the first residue was accomplished using Fmoc-Tyr(tBu)-F according to standard protocol [2]. Briefly, 4-sulfamylbutyryl AM resin (420 mg, 0.33 mmol) (Novabiochem) was swollen for 20 minutes with dry DCM and then drained. A solution of Fmoc-Tyr(tBu)-F ( $\approx 461$  mg, 1 mmol) in dry DCM (2 mL) and di-isopropylethylamine (DIEA) (180  $\mu\text{L}$ , 1 mmol) was added to the drained resin and reacted at 25° C for 1 h. The resin was washed with dry DCM (5 x 5 mL), dried and kept at -20° C until use.

**Chemical synthesis of MCoTI-PMI cyclotides.** Solid-phase synthesis was carried out on an automatic peptide synthesizer ABI433A (Applied Biosystems) using the Fast-Fmoc chemistry with 2-(1H-benzotriazol-1-yl)-1,1,3,3-tetramethyluronium hexafluorophosphate (HBTU) activation protocol at 0.1 mmole scale on a Fmoc-Tyr(tBu)-sulfamylbutyryl AM resin. Side-chain protection was employed as previously described for the synthesis of peptide  $\alpha$ -thiesters by the Fmoc-protocol [3], except for the N-terminal Cys residue, which was introduced as Boc-Cys(Trt)-OH. After chain assembly, the alkylation, thiolytic cleavage and deprotection were performed as previously described [3, 4]. Briefly,  $\approx 100$  mg of protected peptide resin were first alkylated two times with  $\text{ICH}_2\text{CN}$  (174  $\mu\text{L}$ , 2.4 mmol; previously filtered through basic silica) and DIEA (82  $\mu\text{L}$ , 0.46 mmol) in N-methylpyrrolidone (NMP) (2.2 mL) for 12 h. The resin was then washed with NMP (3 x 5 mL) and DCM (3 x 5 mL). The alkylated peptide resin was cleaved with  $\text{HSCH}_2\text{CH}_2\text{CO}_2\text{Et}$  (200  $\mu\text{L}$ , 1.8 mmol) in the presence of a catalytic amount of sodium thiophenolate (NaSPh, 3 mg, 22  $\mu\text{mol}$ ) in dimethylformamide (DMF):DCM (3:4 v/v, 1.4 mL) for 24 h. The resin was then dried at reduced pressure. The side-chain protecting groups were removed by treating the dried resin with trifluoroacetic acid (TFA): $\text{H}_2\text{O}$ :tri-isopropylsilane (TIS) (95:2:3 v/v, 5 mL) for 3-4 h at room temperature. The resin was filtered and the linear peptide thioester was precipitated in cold  $\text{Et}_2\text{O}$ . The crude material was dissolved in the minimal amount of  $\text{H}_2\text{O}$ :MeCN (4:1) containing 0.1% TFA and characterized by HPLC and ES-MS. Cyclization and folding was accomplished by flash dilution of the corresponding MCoTI-PMI linear  $\alpha$ -thioester TFA crudes to a final concentration of  $\approx 50$   $\mu\text{M}$  into freshly degassed 2 mM reduced glutathione (GSH), 50 mM sodium phosphate buffer at pH 7.5 for 18 h. Folded peptides were purified by semi-preparative HPLC using a linear gradient of 25-45% solvent B over 30 min. Pure peptides were characterized by HPLC and ES-MS (Figure S1 and Table S1).

**Construction of cyclotide expressing plasmids.** Plasmids expressing the MCo-PMI cyclotides were constructed using the pTXB1 expression plasmid (New England Biolabs), which contain an engineered Mxe Gyrase intein, respectively, and a chitin-binding domain (CBD). Oligonucleotides coding for the different MCo-PMI variants (Table S2) were synthesized, phosphorylated and PAGE purified by IDT DNA. Complementary strands were annealed in 20 mM sodium phosphate, 300 mM NaCl and the resulting double stranded DNA (dsDNA) was purified using Qiagen's (Valencia, CA) miniprep column and buffer PN. pTXB1 plasmids was double digested with *Nde*I and *Sap*I (NEB). The linearized vectors and the MCoTI-I encoding dsDNA fragments were ligated at 16° C overnight using T4 DNA Ligase (New England Biolabs). The ligated plasmids were transformed into DH5 $\alpha$  cells (Invitrogen) and plated on Luria Broth (LB)-agar containing ampicillin. Positive colonies were grown in 5 mL LB containing ampicillin at 37°C overnight and the corresponding plasmids purified using a Miniprep Kit (Qiagen). Plasmids expressing the MCo-PMI cyclotide precursors with an N-terminal TEV recognition sequence (Met-Glu-Asn-Leu-Tyr-Phe-Gln) were cloned as follows. The DNA encoding TEV N-terminal recognition sequence was generated by PCR using the corresponding MCo-PMI-pTXB1 plasmid. The 5' primer (5'- AAA CAT ATG GAA AAC CTG TAC TTC CAG TGC GGT TCT GGT TCT GG-3') encoded an *Nde* I restriction site. The 3' oligonucleotide (5'-GAT TGC CAT GCC GGT CAA GG-3') introduced a *Spe* I restriction site during the PCR reaction. The PCR amplified product was purified, digested simultaneously with *Nde* I and *Spe* I and then ligated into an *Nde* I- and *Spe* I-treated plasmid pTXB-1 (New England Biolabs). The linearized vectors and the TEV-MCo-PMI encoding dsDNA fragments were ligated at 16°C overnight as described above. The ligated plasmids were transformed into DH5 $\alpha$  cells and screened as described above. The DNA sequence of all the plasmids was confirmed by sequencing.

**Expression and purification of recombinant MCo-PMI cyclotides.** BL21(DE3) (Novagen) were transformed with MCo-PMI encoding plasmids (see above). Expression was carried out in LB medium (1 L) containing ampicillin (100  $\mu$ g/mL) at 30°C for 4 h respectively. Briefly, 5 mL of an overnight starter culture derived from either a single clone or single plate were used to inoculate 1 L of LB media. Cells were grown to an OD at 600 nm of  $\approx$  0.6 at 37° C, and expression was induced by the addition of isopropyl- $\beta$ -D-thiogalactopyranoside (IPTG) to a final concentration of 0.3 mM at 30° C for 4 h. The cells were then harvested by centrifugation. For fusion protein purification, the cells were resuspended in 30 mL of lysis buffer (0.1 mM EDTA, 1 mM PMSF, 50 mM sodium phosphate, 250 mM NaCl buffer at pH 7.2 containing 5% glycerol) and lysed by sonication. The lysate was clarified by centrifugation at 15,000 rpm in a Sorval SS-34 rotor for 30 min. The clarified supernatant was incubated with chitin-beads (2 mL

beads/L cells) (New England Biolabs), previously equilibrated with column buffer (0.1 mM EDTA, 50 mM sodium phosphate, 250 mM NaCl buffer at pH 7.2) at 4°C for 1 h with gentle rocking. The beads were extensively washed with 50 bead-volumes of column buffer containing 0.1% Triton X100 and then rinsed and equilibrated with 50 bead-volumes of column buffer. For the purification of TEV-MCo-PMI-intein-CBD fusion proteins, the beads were washed with 50 bead-volumes of TEV reaction buffer (50mM Tris•HCl, 0.5mM EDTA pH 8.0). Proteolytic cleavage of the TEV sequence was performed on the column by complementing the buffer with 3 mM reduced GSH and adding TEV protease to a final concentration of  $\approx$  0.1 mg/mL. The proteolytic reaction was kept at 4° C overnight with gentle rocking. Once the proteolytic step was completed, the column was then washed with 50-bead volumes of column buffer. Chitin beads containing the different purified MCo-PMI-Intein-CBD fusion proteins were cleaved with 50 mM GSH in degassed column buffer. The cleavage reactions were kept for up to 1-2 days at 25°C with gentle rocking. Once the cleavage reaction was complete, the supernatant of the cleavage reaction was separated by filtration and the beads were washed with additional column buffer to reach a final concentration of 5 mM GSH, and the folding was allow to proceed with gently rocking at 4° C for 48 h. Folded MCo-PMI cyclotides were purified by semipreparative HPLC using a linear gradient of 25-45% solvent B over 30 min. Purified MCoTI-PMI cyclotides were characterized by C18-RP-HPLC and ES-MS (Fig. S1); and quantified by UV-vis spectroscopy (Table S1).

**Refolding of TEV-MCo-PMI-intein-CBD constructs from inclusion bodies.** Inclusion bodies were first washed with column buffer containing 0.2% Triton X (50 mL) and then just column buffer (3 x 50 mL). The pellet was dissolved in 50 mM sodium phosphate and 250 mM NaCl, 8 M urea buffer at pH 7.2 (10 mL). After centrifugation at 15,000 rpm in a Sorval SS-34 rotor the supernatant was slowly flash diluted in 0.1mM EDTA, 50 mM sodium phosphate and 250 mM NaCl, 0.5 M Arg•HCl buffer at pH 7.2. This solution was dialyzed against column buffer (2 L) at 4° C for 2 days. The dialyzed solution was centrifuged at 15,000 rpm for 20 min in a Sorval SS-34 rotor and the supernatant was purified by affinity chromatography on chitin beads. TEV-MCo-PMI-intein-CBD constructs were treated as described above to remove the TEV-leading signal and induce backbone cyclization/folding of the MCo-PMI cyclotides.

**Expression of <sup>15</sup>N-labeled MCo-PMI.** Expression was carried out using BL21(DE3) cells as described above except grown in M9 minimal medium containing 0.1% <sup>15</sup>NH<sub>4</sub>Cl as the nitrogen source. Cyclization and folding was performed in solution as described above. <sup>15</sup>N-labeled MCo-PMI was purified by semipreparative HPLC as before. Purified products were characterized by HPLC and ES-MS (Fig. S2).

**Preparation of FITC-labeled MCo-PMI cyclotides.** MCo-PMI-K37R and MCo-PMI-K37R-F42A were prepared either by chemical synthesis or recombinant expression as described above. The pTXB1-TEV-MCo-PMI-K37R and pTXB1-TEV-MCo-PMI-K37R-F42A plasmids were prepared by mutagenesis using pTXB1-TEV-MCo-PMI or pTXB1-TEV-MCo-PMI-F42A plasmids as template, respectively, and the forward primer (5' - T GGT GCT TCT CGT GCT CCG ACC TC - 3') and reverse primer (5' - G AGG TCG GAG CAC GAG AAG CAC CA - 3') in both cases. MCoTI-PMI-K37R and MCo-PMI-K37R-F42A were purified and characterized as described before (Table S1 and Fig. S1). MCo-PMI cyclotides (100 µg) were mixed with 5 times excess FITC (molar ratio) in 0.1 M sodium bicarbonate buffer at pH 9.0. Reaction was carried out at room temperature in the dark for 2 h. The labeling reaction was quenched with diluted AcOH and the labeled cyclotide purified by C18 Semi-prep HPLC using a linear gradient of 10-45% solvent B over 30 min. Pure labeled peptide was characterized by HPLC and ES-MS (Table S1 and Fig. S1).

**TEV protease expression and purification.** BL21(DE3) cells were transformed plasmid pRK793, which encodes His-tagged TEV protease (Addgene). Expression was carried out in 1 L of LB medium containing ampicillin (100 µg/mL) and chloramphenicol (34 µg/mL) at 30°C for 4 h. Briefly, 5 mL of an overnight starter culture derived from a single clone was used to inoculate 1 L of LB media. Cells were grown to an OD at 600 nm of  $\approx 0.6$  at 37°C, and expression was induced by the addition of IPTG to a final concentration of 1 mM at 30° C overnight. The cells were harvested by centrifugation, resuspended in 30 mL of lysis buffer (0.1 mM PMSF, 10 mM imidazole, 50 mM sodium phosphate, 300 mM NaCl buffer at pH 8.0 containing 5% glycerol) and lysed by sonication. The lysate was clarified by centrifugation at 15,000 rpm in a Sorval SS-34 rotor for 30 minutes. The clarified supernatant was incubated with 1 mL of Ni-NTA agarose beads (Qiagen) previously equilibrated with Ni-NTA column buffer (20 mM imidazole, 50 mM sodium phosphate, 300 mM NaCl buffer at pH 8.0) at 4°C for 1 hour with gentle rocking. The Ni-NTA agarose beads were washed sequentially with Ni-NTA column buffer (2 x 100 mL). The fusion protein was eluted with Ni-NTA elution buffer (50 mM sodium phosphate, 250mM imidazole, 300 mM NaCl, buffer at pH 8) and immediately dialyzed in TEV-protease storage buffer (1 mM EDTA, 5 mM DTT, 50mM Tris•HCl buffer at pH7.5 containing 50% (v/v) glycerol and 0.1% (w/v) Triton X-100). The purity of the TEV protease was checked by SDS-PAGE.

**Cloning and expression of fluorescent protein YPet-p53.** The DNA encoding the fluorescent protein YPet was isolated by PCR using the plasmid pBAD-6 [5] as a template. The forward (5'-AAA AGG ATC CGA TGT CTA AAG GTG-3') and reverse (5'-TTT TGA GCT CTT TGT ACA ATT CAT TC-3') primers contained a BamHI and SacI restriction site, respectively. The resulting

amplicon was purified using Qiagen's PCR purification kit, digested and ligated into *BamH* I- and *SacI*-treated plasmid pRSF-DUET-1 (Novagen) to give T7 expression vector pRSF-YPet. The resulting plasmid was sequenced and shown to be free of mutations. 5'-Phosphorylated synthetic DNA oligos (IDT) (5'-C GGT GGT TCT GGT GGT TCT GGT GGT TCT GGT GGT TCT GGT GGT TCT CTG CAG AGT CAG GAA ACA TTT TCA GAC CTA TGG AAA CTA CTT CCT GAA AAC TAA G-3' and 5'-TC GAC TTA GTT TTC AGG AAG TAG TTT CCA TAG GTC TGA AAA TGT TTC CTG ACT CTG CAG AGA ACC ACC AGA ACC ACC AGA ACC ACC AGA ACC ACC AGA ACC ACC GAG CT-3') encoding a flexible linker (Gly-Gly-Ser)<sub>5</sub> fused in frame to the DNA encoding human p53 (15-29 aa) were annealed and ligated into pRSF-YPet using the *Sac* I and *Sal* I restriction sites to give pRSF-YPet-p53. The resulting plasmid was sequenced and shown to be free of mutations. BL21(DE3) cells (Novagen) (1L) transformed with pRSF-YPet-p53 plasmid were grown to mid-log phase (OD at 600 nm ≈ 0.6) in LB medium containing kanamycin (34 µg/L) at 37° C and then induced with 1 mM IPTG at 30°C for 4 hours. Cells were harvested, lysed and YPet-p53 purified by Ni-affinity chromatography as described above. YPet-p53 protein was eluted with 50 mM sodium phosphate, 250 mM imidazole, 300 mM NaCl buffer at pH 8.0 containing 30% glycerol. The purified proteins were immediately dialyzed against the same buffer with no imidazole and stored at -80° C until use. The purified protein was characterized by SDS-PAGE and ES-MS (Fig. S4)

**Cloning and expression of CyPet-Hdm2.** The DNA encoding the fluorescent protein CyPet was isolated by PCR using the plasmid pBAD-6 [5] as a template. The forward (5'-AAA AGG ATC CAA TGT CTA AAG GTG AAG-3') and reverse (5'- TTT TGA GCT CTT TGT ACA ATT CAT -3') primers contained a *BamH* I and *Sac* I restriction site, respectively. The resulting amplicon was purified using Qiagen's PCR purification kit, digested and ligated into *BamH* I- and *Sac* I-treated plasmid pRSF-DUET-1 (Novagen) to give T7 expression vector pRSF-CyPet. The resulting plasmid was sequenced and shown to be free of mutations. The DNA encoding the p53 binding domain of the human homolog of Mdm2 (Hdm2, residues 17-125) was isolated by PCR using the cDNA for Hdm2 (accession number: BT007258) as template. The forward primer (5'-T GCA CTG CAG TCA CAG ATT CCA GCT TCG GAA C-3') encoded a *Pst* I restriction site. The reverse primer (5'- GC GTCGAC TTA GTT CTC ACT CAC AGA TGT ACC TGA-3') encoded a *Sal* I site and a stop codon. The resulting amplicon was purified using Qiagen's PCR purification kit, digested and ligated into *Pst* I- and *Sal* I-treated plasmid pRSF-CyPet to give T7 expression vector pRSF-CyPet-Hdm2. The resulting plasmid was sequenced and shown to be free of mutations. BL21(DE3) cells (Novagen) (1L) transformed with pRSF-CyPet-Hdm2 plasmid were grown to mid-log phase (OD at 600 nm ≈ 0.6) in LB medium

containing kanamycin (34 µg/mL) at 37° C and then induced with 1 mM IPTG at 30°C for 4 h. Cells were harvested, lysed and CyPet-Hdm2 purified by Ni-affinity chromatography and stored as described before for YPet-p53. Purified CyPet-Hdm2 was characterized by SDS-PAGE and ES-MS (Fig. S4).

**Cloning and expression of CyPet-HdmX.** The DNA encoding the p53 binding domain of the human homolog of MdmX (HdmX, residues 17-116) was isolated by PCR using the cDNA for HdmX (accession number: BC105106) as a template. The forward primer (5'- T GCA CTGCAG TGC AGG ATC TCT C-3') encoded a *Pst* I restriction site. The reverse primer (5'- GC GTC GAC TTA AGC ATC TGT AGT AGC AGT-3') encoded a *Sal* I site and a stop codon. The resulting amplicon was purified using Qiagen's PCR purification kit, digested and ligated into *Pst*I- and *Sal*I-treated plasmid pRSF-CyPet to give T7 expression vector pRSF-CyPet-HdmX.

Rosetta(DE3) cells (Novagen) (1L) transformed with pRSF-CyPet-HdmX plasmid were grown to mid-log phase (OD at 600 nm ≈ 0.6) in LB medium containing kanamycin (34 mg/L) and chlorophenical (34 µg/mL) at 37° C and then induced with 1 mM IPTG at 30° C for 4 ho. Cells were harvested, lysed and CyPet-HdmX purified by Ni-affinity chromatography and stored as described above for YPet-p53. Purified CyPet-Hdm2 was characterized by SDS-PAGE and ES-MS (Fig. S4).

**Cloning and expression of Hdm2 (17-125).**The DNA encoding the p53 binding domain of Hdm2 (residues 17-125) was isolated by PCR using the cDNA for Hdm2 (accession number: BT007258) as template. The forward (5'-AAA ACA TAT GTC ACA GAT TCC AGC TTC G-3') and reverse (5'-AAA AGG ATC CTT AGT TCT CAC TCA CAG ATG -3') primers contained an *Nde* I and *Bam*H I restriction site, respectively. The resulting amplicon was purified using Qiagen's PCR purification kit, digested and ligated into *Nde* I- and *Bam*H I-treated plasmid pET28a (Novagen) to give T7 expression vector pET28-Hdm2. The resulting plasmid was sequenced and shown to be free of mutations. BL21(DE3) cells (1L) transformed with pET28-Hdm2 plasmid were grown to mid-log phase (OD<sub>600</sub> ≈ 0.6) in LB medium containing kanamycin (34 µg/mL) at 37° C and then induced with 1 mM IPTG at 30° C for 4 h. Cells were lysed and the protein purified by Ni-affinity chromatography as described above. Hdm2 (17-125) was dialyzed against PBS buffer (50 mM sodium phosphate and 150 mM NaCl pH 7.2 containing 30% glycerol) and immediately used.

**Cloning and expression of HdmX (17-116).** The DNA encoding the p53 binding domain of the human homolog of MdmX (HdmX, residues 17-116) was isolated by PCR using the cDNA for HdmX (accession number: BC105106) as a template. The forward (5'-ATT AGG ATC CTG CAG GAT CTC TCC TGG ACA AAT C-3') and reverse (5'- ATT AAA GCT TCT ACT AAG CAT CTG

TAG TAG CAG TGG CTA AAG TG -3') primers contained a *BamH* I and *Hind* III restriction site, respectively. The resulting amplicon was purified using Qiagen's PCR purification kit, digested and ligated into *BamH* I- and *Hind* III-treated plasmid pET28a (Novagen) to give T7 expression vector pET28-HdmX. The resulting plasmid was sequenced and shown to be free of mutations. BL21(DE3) cells (1L) transformed with pET28-HdmX plasmid were grown to mid-log phase (OD at 600 nm  $\approx$  0.6) in LB medium containing kanamycin (34  $\mu$ g/mL) at 37° C and then induced with 1 mM IPTG at 30° C for 4 h. Cells were lysed and the protein purified by Ni-affinity chromatography as described above. HdmX (17-116) was dialyzed against PBS buffer (50mM sodium phosphate and 150mM NaCl pH 7.2) and further purified by gel filtration chromatography on a Superdex-75 column in PBS buffer. Pure fractions were pooled, re-concentrated in 50mM sodium phosphate and 150mM NaCl pH 7.2 and immediately used.

**Expression of  $^{15}\text{N}$ ,  $^{13}\text{C}$ -labeled Hdm2 (17-125).** Expression was carried out using BL21(DE3) cells as described above except grown in M9 minimal medium containing 0.1%  $^{15}\text{NH}_4\text{Cl}$  and 0.2%  $^{13}\text{C}_6\text{-D-glucose}$  as the nitrogen and carbon sources, respectively. Protein purification was performed as described above. Protein was characterized by ES-MS (Fig. S5).

**NMR spectroscopy.** NMR samples were prepared by dissolving  $^{13}\text{C}$ - and/or  $^{15}\text{N}$ -labeled peptides/proteins into 80 mM potassium phosphate in 90%  $\text{H}_2\text{O}/10\%$   $^2\text{H}_2\text{O}$  (v/v) or 100%  $\text{D}_2\text{O}$  to a concentration of approximately 0.2 mM and molar ratio of 1:1 between MCo-PMI and Hdm2 with the pH adjusted to 6.5 by addition of dilute HCl. All NMR data were recorded on a Bruker Avance II 700 MHz spectrometer equipped with a cryoprobe. Data were acquired at 27 °C, and 2,2-dimethyl-2-silapentane-5-sulfonate, DSS, was used as an internal reference. All 3D experiments, HNCA, HNCACB, CBCACONH, HBHACONH,  $^1\text{H}\{^{15}\text{N}\}$ -TOCSY-HSQC  $^1\text{H}\{^{13}\text{C}\}$ -NOESY-HSQC and  $^1\text{H}\{^{15}\text{N}\}$ -NOESY-HSQC [6], were performed according to standard procedures [7] with spectral widths of 12 ppm in proton dimensions, 70 or 35 ppm in carbon dimension, and 35 ppm in nitrogen dimension. The carrier frequency was centered on the water signal, and the solvent was suppressed by using WATERGATE pulse sequence. TOCSY (spin lock time 80 ms) and NOESY (mixing time 150 ms) spectra were collected using 1024  $t_3$  points, 256  $t_2$  and 128  $t_1$  blocks of 16 transients. Spectra were processed using Topspin 2.1 (Bruker). Each 3D-data set was apodized by 90°-shifted sinebell-squared in all dimensions, and zero filled to 1024 x 512 x 256 or 1024x256x128 points prior to Fourier transformation. Chemical shifts were assigned by using CARA software [8].

**Structure determination.** Structural calculations were carried out with Cyana 2.1 [9] using 986 distance restraints derived from  $^1\text{H}$ - $^1\text{H}$ -NOESY,  $^{13}\text{C}$ -edited NOESY and  $^{15}\text{N}$ -edited NOESY spectra, 150 pairs of backbone torsion angle restraints derived from TALOS [10], 38 restraints



for hydrogen bonds, and the restraints from three disulfide bond between Cys25 and Cys42, Cys32 and Cys44, and Cys38 and Cys50 of MCo-PMI. To account for cyclic nature of MCo-PMI, amide nitrogen of Gly1 and carbonyl carbon of Cys51 were linked and upper and lower distance restraints between amide proton and nitrogen of Gly1 and carbonyl carbon and oxygen of Cys51 were added [9]. nOes were converted to upper limit distances using the CALIBA module in CYANA [9]. The reference volume determined by CALIBA was increased 2 times before conversion in order to loosen the distance restraints. All upper limit distances for intermolecular nOes were set to 5 Å. Backbone torsion angle restraints for MCo-PMI-Hdm2 were estimated by using the TALOS [10]. These experimental restraints are summarized in Table S3. To perform CYANA calculations, a single polypeptide chain was constructed for the MCo-PMI and Hdm2 molecules.

Refinement: The CYANA-generated structures were subjected to minimization in explicit water by using CHRMM [11] and further analysis by PROCHECK\_NMR [12]. 86.5% of the V domain residues were in the most favorable regions of Ramachandran plot, 13.5% were in the additional allowed regions. There were no residues in generously allowed or the disallowed regions of the Ramachandran plot. The structural statistics of the 10 best structures are reported in Table S3. The solution structure of Hdm2 (17-125) with cyclotide MCo-PMI has been deposited and assigned the RCSB ID code rcsb103330 and PDB ID code 2m86.

**Fluorescence polarization binding assays.** Fluorescence polarization of FITC-labeled MCo-PMI cyclotides upon addition of either Hdm2 (17-125) or HdmX (17-116) was measured at 22°C using a Spex Fluorolog 3 spectrofluorometer (Horiba Scientific) with the excitation bandwidth set at 1 nm and emission at 5 nm. The excitation wavelength for fluorescein was set at 495 nm and emission was monitored at 521 nm. The equilibrium dissociation constant ( $K_D$ ) were obtained by titrating a fixed concentration of FITC-labeled MCo-PMI cyclotide (5 nM) with increasing concentrations of either Hdm2 (17-125) or HdmX (17-116) in 50 mM sodium phosphate, 150 mM NaCl buffer at pH7.2 by assuming formation of a 1:1 complex and using the Prism (GraphPad) software package.

***In vitro* inhibition p53-Hdm2/HdmX competition experiments.** *In vitro* IC<sub>50</sub> values were measured by inhibition competition experiments using the FRET-based reporter formed by CyPet-Hdm2/CyPet-HdmX and YPet-p53. Briefly, a solution of CyPet-Hdm2/HdmX (20 nM) and YPet-p53 (5 μM) in 10 mM phosphate buffer, 150 mM NaCl buffer at pH 7.2 was titrated with increasing amounts of inhibitor (ranging from 0 to 100 μM). The decrease in fluorescence signal at 525 nm (excited at 414 nm) was measured and plotted against the concentration of free

inhibitor. The resulting plot was fitted to a single binding site competition curve using the Prism (GraphPad) software package.

**Cell viability assay.** LNCaP, HCT116 p53<sup>+/+</sup>, HCT116 p53<sup>-/-</sup>, JEG3, DU145, PC3, HEK293T and HBL100 cell lines were cultured in RPMI 1640 medium supplemented with 10% fetal calf serum, penicillin (50 IU/mL) and streptomycin (50 µg/mL) at 37° C in 5% CO<sub>2</sub>. Cell viability was performed using the MTT assay. Briefly,  $\approx 2 \times 10^3$  cells were seeded in 96-well microtiter plates in 100 µL RPMI 1640 in the presence of 10% calf serum. After 24 h incubation the cells were washed with PBS and treated with 30 µL/well of PBS or RPMI 1640 media containing the peptides or Nutlin-3 at the indicated doses for 1 h at 37° C in 5% CO<sub>2</sub>. After 1 h, 210µL/well of full complemented media was added and the cells were grown for 48 h and then treated with 20 µL of a solution of 3-(4,5-dimethylthiazol-2-yl)-2,5-diphenyltetrazolium bromide (MTT, 5 mg/mL) for 2 h. The medium was discarded and DMSO (100 µL/well) was added to each well and incubated with gentle shaking for 20 min at room temperature. The absorbance at 595 nm of the solution was analyzed using a Tecan Genios Multifunctional Microplate Reader (Tecan System Inc) and the background at 670 nm subtracted.

**Cell Cycle Assay.** LNCaP and HCT116 p53<sup>+/+</sup> cells were seeded at a density of  $8 \times 10^4$  cells per well in 12-well plates and grown in RPMI 1640 in the presence of 10% calf serum for 24 h. Cells were washed with PBS and incubated with 300 µL/well of PBS or RPMI 1640 containing the peptides or Nutlin-3 at the indicated doses for 1 h at 37°C in 5% CO<sub>2</sub>. After 1 h, 2.1 mL of full complemented media was added per well and the cells were grown for 24 h, washed twice with ice-cold PBS, trypsinized and resuspended in 0.3 mL of ice-cold PBS at a density of  $\approx 2 \times 10^5$  cells/mL. To this solution 0.7 mL of 100% EtOH was added dropwise with gentle vortexing and stored at 4° C overnight. Cells were washed once with ice-cold PBS, resuspended in PBS containing propidium iodide (10 µg/mL) and DNase-free RNase A (100 µg/mL); and incubated at 37° C for 15 min. The suspension was then analyzed in a FACSAria II (BD Biosciences).

**Caspase-3/7 activation assay.** LNCaP or HCT116 p53<sup>+/+</sup> cells were seeded in 96-well plates at a density of  $\approx 2 \times 10^3$  cells and treated with vehicle, Nutlin 3 (EMD Chemicals) (20 µM), MCo-PMI (50 µM) or MCo-PMI-F43A (50 µM) as described before for the cell cycle analysis assay. After 24 h of treatment, caspase-3/7 activity was measured by addition of Caspase-Glo 3/7 chemiluminescence reagent (Promega) according to the manufacturer's protocol and the luminescence was measured using a Synergy H1 Hybrid Multi-Mode Microplate Reader (BioTek).

**Co-immunoprecipitation analysis.** LNCaP or HCT116 p53<sup>+/+</sup> cells ( $\approx 1 \times 10^5$ ) were incubated with FITC-labeled MCo-PMI peptides as described above for 1 h. After 30 h of treatment, the

cells were washed three times with 3 mL cold PBS and detached by treatment with trypsin–EDTA (Sigma) at 37° C for 5 min. The cells were harvested in 3 mL cold PBS and pelleted by centrifugation at 600 x g at 4° C for 10 min. In order to remove any peptide bound to membrane the cell pellets were isolated and washed three times with trypsin–EDTA for 5 min, three times with cold PBS containing 0.5 mg/mL of heparin (Sigma), followed by another cold PBS wash [13]. Washed cells were lysed using RIPA buffer (Sigma) containing 1 mM PMSF and EDTA-free Halt protease Inhibitor cocktail (Thermo Scientific). The cell lysate was incubated with 50 µL of protein A/G high capacity agarose beads (Thermo Scientific) for 30 min at 4° C. The supernatant was collected and the proteins were precipitated with mouse-anti-FITC monoclonal IgG antibody (Invitrogen). Western analysis of electrophoresed proteins was performed using mouse anti-Hdm2 (Santa Cruz), rabbit anti-HdmX (Bethyl Laboratories) and mouse anti-GAPDH (Cell signaling). Western blots were visualized by fluorescence imaging using either a Storm 860 (Molecular Dynamics) or a Typhoon 8600 (Molecular Dynamics) imaging system.

**Mice xenografts studies.** HCT116 p53<sup>+/+</sup> xenografts were established by injecting 100 µL suspension of basal RPMI containing  $0.5 \times 10^6$  cells into the rear right flanks of female nude mice (nu/nu) mice (Simonsen Laboratories). When tumors reached an average volume of  $\approx 100$  mm<sup>3</sup>, cohorts (n=3) were treated with vehicle (5% dextrose in water, D5W), MCo-PMI (40 mg/kg, 7.6 mmol/kg), or Nutlin-3 (10 mg/kg, 17.2 mmol/kg) (EMD Chemicals) once daily for up to 38 days by intravenous injection (MCo-PMI and vehicle) or by intraperitoneal administration (Nutlin-3). Compounds were prepared in a D5W at a final volume of 50 µL (peptide) or 100 µL (Nutlin-3). Health checks were performed daily to observe parameters such as body conditioning score, overall appearance and cleanliness, strength of grip, skin color and tone, mobility, gait and activity level as indicators of potential drug related toxicities. Individual weights were recorded thrice weekly (Fig. S7), comparing the control and treatment groups as an additional indicator of tolerance of drug treatment as well as providing the average weight for calculation of drug dosing. Tumor size was measured with calipers. Tumor volume was calculated by measuring tumor size in two dimensions and applying those measurements to the calculation  $V = d^2 \times D/2$ , where d and D equal to the smaller and larger of the two measurements, respectively. Mice bearing tumors larger than 2.4 cm<sup>3</sup> were removed from the study, sacrificed and necropsies performed to gather tumor and organ samples for histological analysis. Tumor and tissue samples were perfused with PBS, after which portions were either fixed in 10% formalin overnight then transferred to 100% EtOH or snap-frozen in liquid nitrogen and stored at -70° C until analysis.

**Quantitative RT-PCR.** HCT116 p53<sup>+/+</sup> subcutaneous tumors were excised, flash frozen and the RNA extracted using the RNeasy Mini kit (QIAGEN). Total RNA was reverse transcribed to cDNA using M-MLV reverse transcriptase (Promega). The generated cDNA was amplified with power SYBR Green PCR master mix (Applied Biosystems) on a 96 well plate and measured the relative transcript levels by qRT-PCR on an ABI 7900HT Fast Real-Time PCR System (Applied Biosystems). Specific primers for *HDM2*, *p21* and the  $\beta$ -*actin* control were used. The amplification reactions were done in triplicate in 96-well optical plates. Threshold-cycle (Ct) values were automatically calculated for each replicate and used to determine the relative expression of the gene of interest relative to  $\beta$ -*actin*.

**Immunohistochemistry.** Formalin-fixed, paraffin-embedded (FFPE) tumor samples were sectioned at a thickness of 5  $\mu$ m and mounted on pre-cleaned, charged glass slides. For immunohistochemistry, tumor sections were de-paraffinized in 3 x 5 min changes of clear-rite 3 (Microm International). Samples were then rehydrated by treatment with 100% ethanol (EtOH) (2 x 10 min) followed by treatment with 95% EtOH in H<sub>2</sub>O (2 x 10 min) and then washed with pure H<sub>2</sub>O. For antigen unmasking, slides were incubated at 95° C in 10 mM sodium citrate buffer containing 0.05 % tween-20 at pH 6.0 for 10 min. The slides were cooled to room temperature and washed 3 x 2 min in phosphate-buffered saline without calcium and magnesium salts (PBS) (3 x 2 min). Immunohistochemical staining was carried out using the Ultravision ONE Detection System (Thermo Scientific) containing horseradish-peroxidase polymer (Thermo Scientific) and DAB Plus Chromagen (Thermo Scientific) according to the manufacturer's directions. Briefly, tissues were incubated with hydrogen peroxide blocking (Thermo Scientific) reagent to quench endogenous peroxides, and then washed with PBS (4 x 2 min). Ultra V blocking agent (Thermo Scientific) was applied to prevent non-specific binding. The corresponding primary antibodies were prepared at a concentration of 1  $\mu$ g/mL in PBS containing 1.5 % normal goat serum. Following overnight incubation at 4° C in the presence of antibody, tissue sections were washed as before and incubated with HRP polymer prior to application of DAB chromagen/substrate. Tissue sections were incubated with DAB for 3 min to allow color to develop. Slides were washed with pure H<sub>2</sub>O (4 x 5 min), counterstained with hematoxylin solution (Microm International) for 1 min and immediately washed with pure H<sub>2</sub>O. Slides were dehydrated with successive washes of 95 % and 100 % EtOH, and clearite-3, then mounted with clarion mounting media (Sigma-Aldrich) and glass coverslips. Slides were air-dried overnight and visualized using Zeiss Axioskop light microscope equipped with 5x and 20x objectives and motic digital camera.

**Human serum stability.** Peptides (150 µg dissolved in 50 µL PBS) were mixed with 500 µL human serum and incubated at 37° C. Aliquot samples (50 µL) were taken at different time points (0-120 h) and precipitated with 20% trichloroacetic acid. After centrifugation the pellet was dissolved in 200 µL of 8 M GdmCl. Both the supernatant and solubilized pellet fractions were analyzed by HPLC and LC-MS/MS. Each experiment was done in triplicate.

**Human serum binding kinetics.** Binding kinetics were carried out at 25 °C on a BLItz™ instrument (ForteBIO), using biotinylated MCo-PMI immobilized onto a streptavidin coated biosensor tip. MCo-PMI (1 mg, 190 nmol) was conjugated with three-fold molar excess of NHS-PEG4-Biotin in 0.1 M sodium phosphate buffer (1.9 mL) at pH 7.4 for 1 h. The reaction was quenched by adding 2% TFA until pH ≈ 4. Purification and desalting of biotinylated MCo-PMI was performed on a Zeba spin desalting columns (Thermo Scientific). Binding of MCo-PMI to human serum proteins was performed at 1/100 and 1/200 serum dilutions in 20 mM sodium phosphate, 100 mM NaCl buffer at pH 7.2, which correspond to a concentration of 25 µM and 50 µM human serum albumin, respectively. Serum proteins were allowed to bind to the MCo-PMI coated biosensor tip for 2 minutes followed by a dissociation step of 2 minutes. Nonlinear regression analysis was performed using Prism (GraphPad Software) to calculate the association ( $k_{on}$ ) and dissociation ( $k_{off}$ ) rates, and corresponding  $K_D$  value.

**Table S1.** Molecular weights and molar absorptivities for the folded cyclotides used in this work.

Peptide Name	Molecular weight (Da)		Molar extinction coefficient ( $M^{-1} \text{ cm}^{-1}$ )
	Expected	Found	
MCo-PMI	5262.0	5262.9 $\pm$ 0.4	8855 <sup>a</sup>
<sup>15</sup> N-MCo-PMI	5329.9	5329.9 $\pm$ 0.2	8855 <sup>a</sup>
MCo-PMI-K37R	5291.3	5290.8 $\pm$ 1.0	8855 <sup>a</sup>
MCo-PMI-F42A	5185.1	5185.8 $\pm$ 0.4	8855 <sup>a</sup>
MCo-PMI-6CIW	5324.2	5324.8 $\pm$ 0.5	8855 <sup>a</sup>
FITC-MCo-PMI-K37R-F42A	5604.0	5603.4 $\pm$ 0.2	70,000 <sup>b</sup>
FITC-MCo-PMI-K37R	5678.3	5679 $\pm$ 1	70,000 <sup>b</sup>
FITC-MCo-6CIW	5713.6	5713.3 $\pm$ 0.5	70,000 <sup>b</sup>

<sup>a</sup> 280 nm, pH 7.4<sup>b</sup> 494 nm, pH 8.0**Table S2.** Forward (p5) and reverse (p3) 5'-phosphorylated oligonucleotides used to clone the different MCo-PMI linear precursors into the pTXB1 expression plasmid.

Cyclotide name	Oligonucleotide sequence	
MCo-PMI	p5	5' -TATGTGCGGTTCTGGTTCTGGTGCTTCTAAAGCTCCGACCTCTTTGCTGAATAC TGGAACCTGCTGTCTGCTGGTGGTGTGTTGCCCGAAAAATCCTGCAGCGTTGCCGTCGTG ACTCTGACTGCCCGGGTCTTGCATCTGCCGTGGTAACGGTTAC-3'
	p3	5' -GCAGTAACCGTTACCACGGCAGATGCAAGCACCCGGGCAGTCAGAGTCACGACGG CAACGCTGCAGGATTTTCGGGCAAACACCACCAGCAGACAGCAGGTTCCAGTATTCAG CGAAAGAGGTCGGAGCTTTAGAAGCACCAGAACCAGAACCAGCACA-3'
MCo-PMI-F42A	p5	5' -TATGTGCGGTTCTGGTTCTGGTGCTTCTAAAGCTCCGACCTCTGCTGCTGAATAC TGGAACCTGCTGTCTGCTGGTGGTGTGTTGCCCGAAAAATCCTGCAGCGTTGCCGTCGTG ACTCTGACTGCCCGGGTCTTGCATCTGCCGTGGTAACGGTTAC-3'
	p3	5' - GCAGTAACCGTTACCACGGCAGATGCAAGCACCCGGGCAGTCAGAGTCACGACGG CAACGCTGCAGGATTTTCGGGCAAACACCACCAGCAGACAGCAGGTTCCAGTATTCAG CAGCAGAGGTCGGAGCTTTAGAAGCACCAGAACCAGAACCAGCACA -3'

**Table S3.** Tabulation of chemical shift differences of backbone amide nitrogen ( $^{15}\text{N}^{\alpha}$ ) and proton ( $\text{H-N}^{\alpha}$ ) between free MCo-PMI and MCoTI.

Residue Number	MCo-PMI		$\Delta \delta$ [MCo-PMI – MCoTI-I]	
	$\delta \text{H-N}^{\alpha}$ / ppm	$\delta ^{15}\text{N}^{\alpha}$ / ppm	$\Delta \delta \text{H-N}^{\alpha}$ / ppm <sup>1</sup>	$\Delta \delta ^{15}\text{N}^{\alpha}$ / ppm <sup>1</sup>
G1	7.953	106.813	-0.127	-1.623
G2	8.051	107.411	-0.001	-3.381
V3	7.784	117.804	-0.548	-3.156
C4	8.699	125.132	0.158	-1.263
K6	8.079	120.638	-0.017	0.03
I7	7.521	121.335	-0.002	1.367
L8	8.567	127.726	0.039	1.941
C11	8.168	126.382	-0.176	6.039
R12	7.965	117.19	-0.011	0.016
R13	9.253	117.392	-0.107	-0.443
D14	9.048	124.221	0.018	0.119
S15	8.183	115.05	-0.089	-0.699
D16	7.628	120.483	-0.023	-0.085
C17	7.761	117.333	-0.21	-0.41
G19	8.397	106.99	0.03	0.358
A20	8.187	124.766	-0.142	-0.373
C21	8.133	117.292	0.07	0.29
I22	8.843	113.765	-0.059	0.421
C23	9.252	120.79	-0.074	-0.15
R24	7.984	128.329	-0.033	-0.251
G25	8.864	108.46	0.063	0.184
N26	7.651	115.703	-0.042	-0.065
G27	8.285	107.257	-0.007	-0.069
Y28	7.16	116.506	-0.028	-0.154
C29	8.646	119.966	-0.032	-0.77
G30	9.658	109.284	-0.055	-0.385
S31	8.611	115.314	-0.097	-0.499
G32	8.848	110.885	-0.217	-0.842
S33	8.29	115.361	-0.291	-0.682

<sup>1</sup> Chemical shift differences between the common residues (1-33) of MCo-PMI and MCoTI-I.

**Table S4.** Tabulation of chemical shift differences of backbone amide nitrogen ( $^{15}\text{N}^{\alpha}$ ) and proton ( $\text{H-N}^{\alpha}$ ) between free MCo-PMI and Hdm2-bound MCo-PMI.

Residue Number	Hdm2-bound MCo-PMI		$\Delta \delta$ [Hdm2-bound MCo-PMI – free MCo-PMI]	
	$\delta \text{H-N}^{\alpha}$ / ppm	$\delta ^{15}\text{N}^{\alpha}$ / ppm	$\Delta \delta \text{H-N}^{\alpha}$ / ppm <sup>1</sup>	$\Delta \delta ^{15}\text{N}^{\alpha}$ / ppm <sup>1</sup>
G1	7.879	106.566	-0.074	-0.247
G2	8.033	107.532	-0.018	0.121
V3	7.95	117.804	0.166	0
C4	8.748	125.3	0.049	0.168
K6	8.125	120.668	0.046	0.03
I7	7.55	121.619	0.029	0.284
L8	8.593	128.057	0.026	0.331
Q9	8.817	126.353	0.01	0.163
R10	8.659	127.641	0.005	0.055
C11	8.149	126.18	-0.019	-0.202
R12	7.952	117.135	-0.013	-0.055
R13	9.221	117.368	-0.032	-0.024
D14	9.062	124.25	0.014	0.029
S15	8.009	111.255	-0.174	-3.795
D16	7.592	120.379	-0.036	-0.104
C17	7.686	117.086	-0.075	-0.247
G19	8.425	107.269	0.028	0.279
A20	8.198	125.64	0.011	0.874
C21	8.167	117.393	0.034	0.101
I22	8.879	114.105	0.036	0.34
C23	9.26	120.771	0.008	-0.019
R24	7.988	128.339	0.004	0.01
G25	8.891	108.569	0.027	0.109
N26	7.648	115.75	-0.003	0.047
G27	8.275	107.292	-0.01	0.035
Y28	7.17	116.57	0.01	0.064
C29	8.631	119.842	-0.015	-0.124
G30	9.644	109.31	-0.014	0.026
S31	8.648	115.471	0.037	0.157
G32	8.891	110.844	0.043	-0.041
S33	8.32	115.464	0.03	0.103
G34	8.571	107.189	0.362	-4.871
A35	9.225	122.629	1.135	11.148
S36	8.291	119.024	0.488	2.976
K37	8.321	127.76	-0.072	5.377
A38	8.2	125.595	0.039	3.011
T40	8.107	111.647	0.291	-3.002
S41	8.216	115.52	0.288	-4.255



F42	8.877	123.128	1.051	4.471
A43	8.068	123.71	0.319	2.563
E44	7.934	122.703	0.084	2.086
Y45	7.394	116.589	-0.414	-3.517
W46	7.996	118.49	0.149	0.816
N47	8.47	110.763	0.248	-4.871
L48	8.449	111.233	0.343	-11.592
L49	7.456	113.116	-0.306	-11.105
S50	8.003	111.251	-0.439	0.04
A51	7.442	123.375	-0.583	-0.255

---

<sup>†</sup> Chemical shift differences between Hdm2-bound and free MCo-PMI.

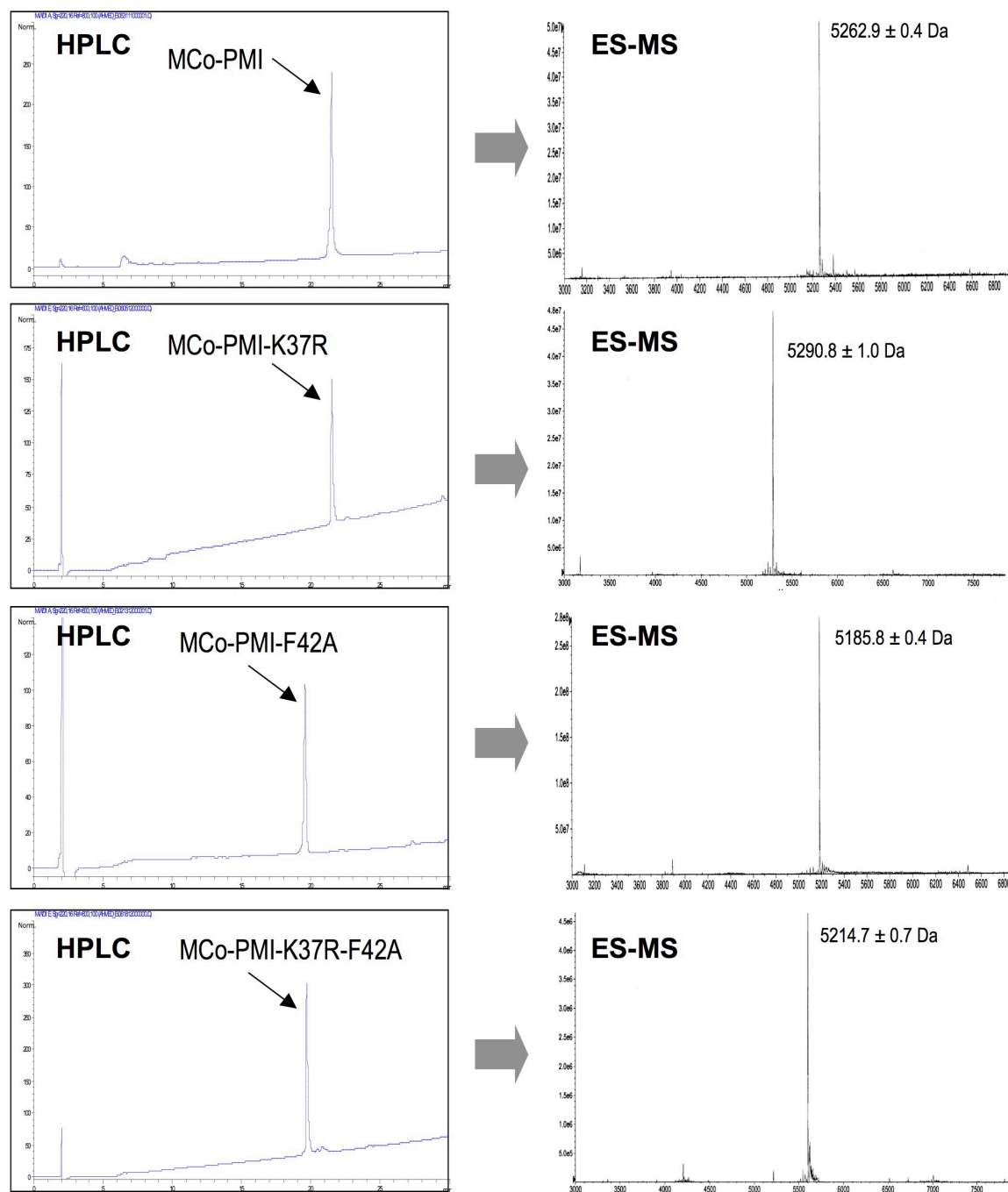


**Figure S1.** Analytical reverse-phase C18-HPLC traces and electro spray mass spectra (deconvoluted) of purified MCo-PMI cyclotides. HPLC analysis was performed using a linear gradient of 0-70% solvent B over 30 minutes.

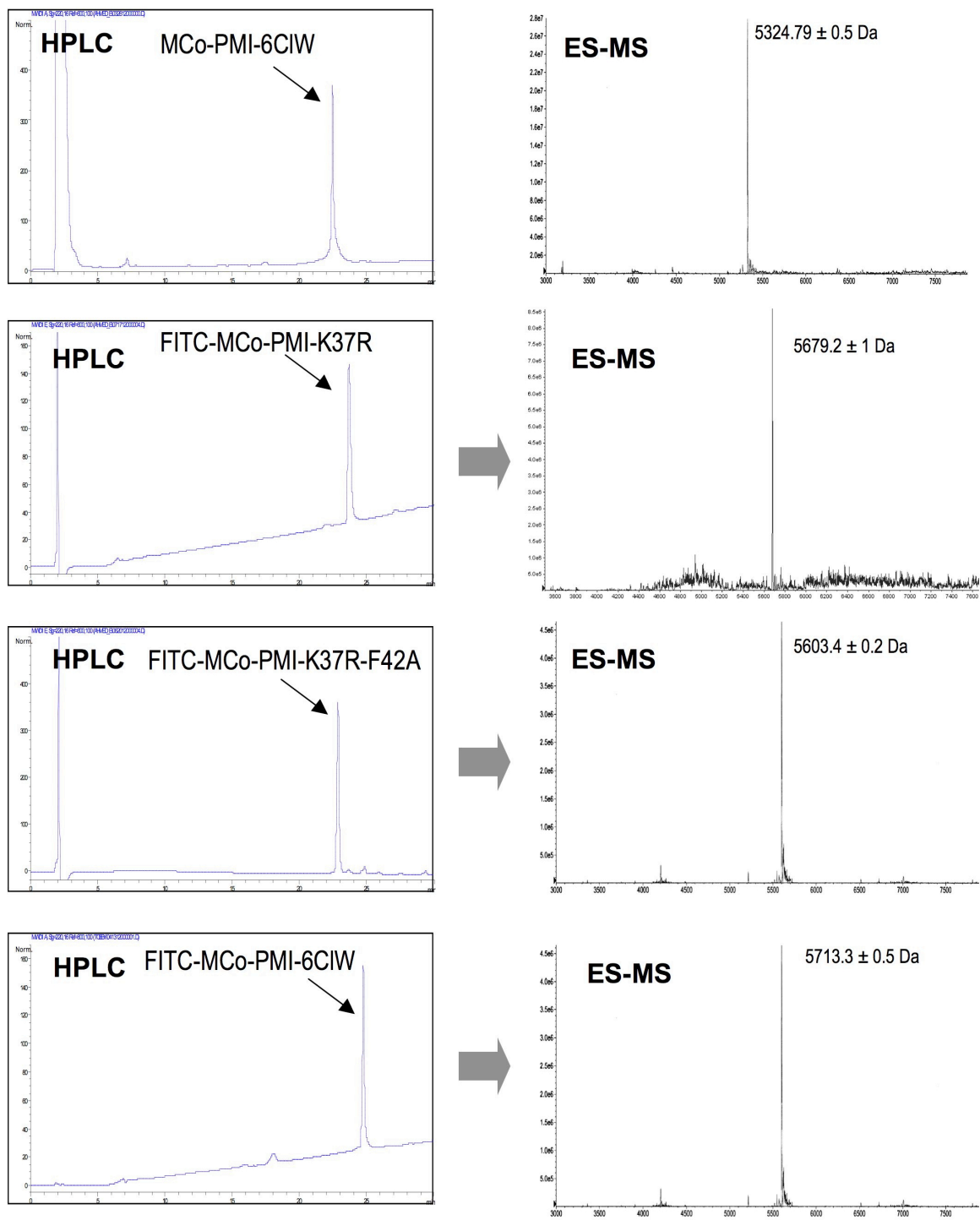
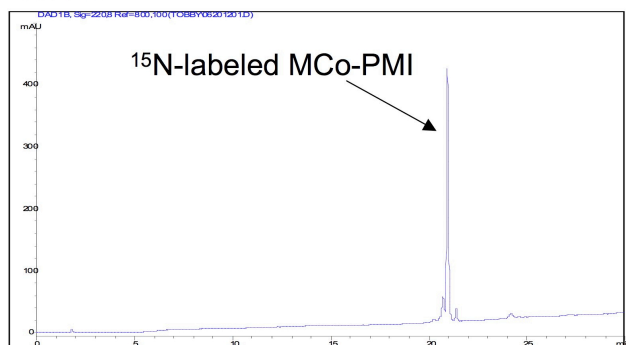


**Figure S1 (Cont.).** Analytical reverse-phase C18-HPLC traces and electrospray mass spectra (deconvoluted) of purified MCo-PMI cyclotides. HPLC analysis was performed using a linear gradient of 0-70% solvent B over 30 minutes.

### HPLC



### ES-MS

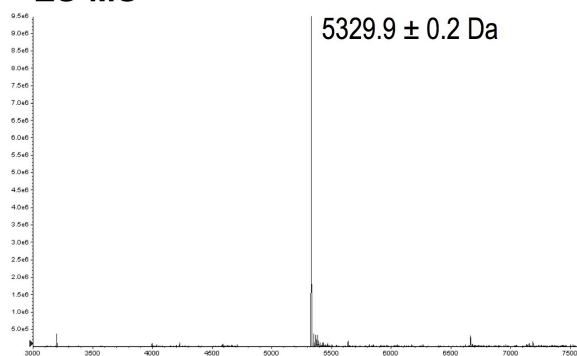


**Figure S2.** Analytical reverse-phase C18-HPLC traces and electrospray mass spectra (deconvoluted) of purified <sup>15</sup>N-labeled MCo-PMI cyclotide. HPLC analysis was performed using a linear gradient of 0-70% solvent B over 30 minutes.

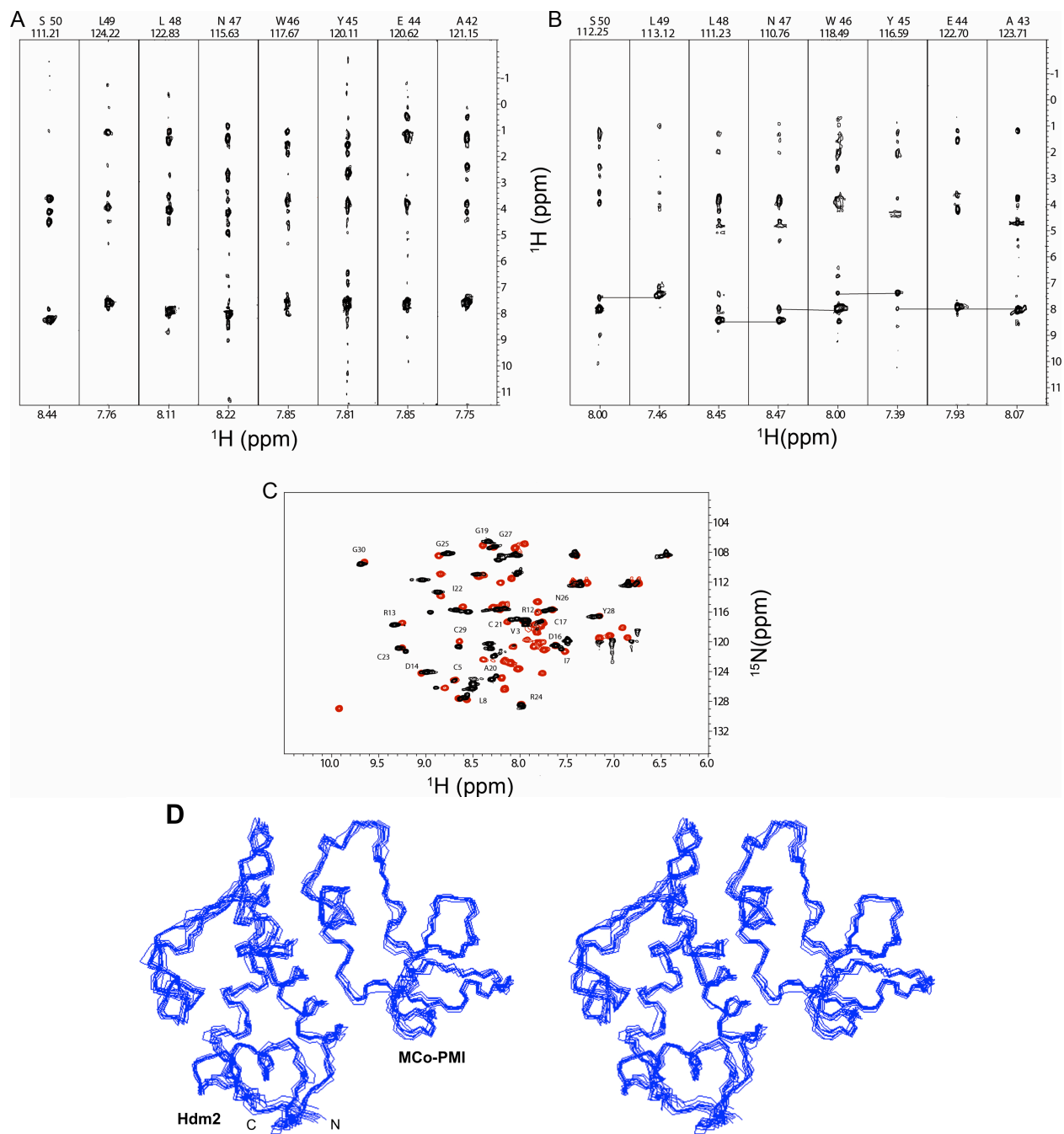


**Figure S3.** NMR analysis of MCo-PMI. **A.** Selected  $F_1(^1\text{H})$ - $F_3(^1\text{H}^\alpha)$  regions from a 3D  $^1\text{H}$ - $^{15}\text{N}$  NOESY HSQC spectrum of free MCo-PMI in solution. **B.** Selected  $F_1(^1\text{H})$ - $F_3(^1\text{H}^\alpha)$  regions from a 3D  $^1\text{H}$ - $^{15}\text{N}$  NOESY HSQC spectrum of MCo-PMI bound to Hdm2 in solution shows  $\alpha$  helical pattern characteristics. **C.** Overlay of HSQC spectra of MCoTI-I (black) and MCo-PMI (red) in solution. **D.** Backbone superposition of ten energy minimized structures of MCo-PMI Hdm2 bound complex.

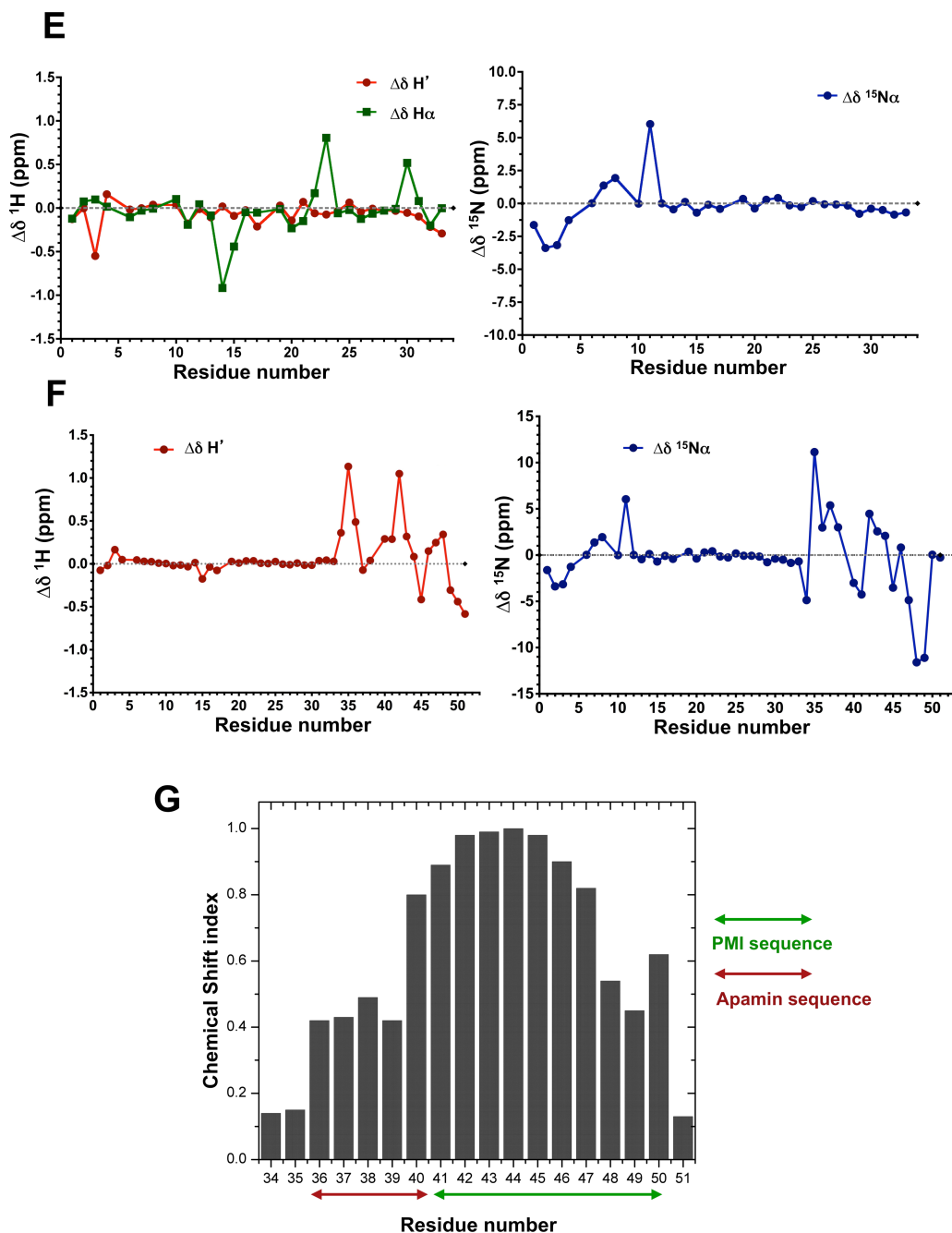


**Figure S3 (cont.). E.** Changes in the backbone protons ( $\text{H-N}^\alpha$  ( $\text{H}'$ ) and  $\text{H}^\alpha$ ) and  $\text{N}^\alpha$  chemical shifts between the common sequence of MCoTI-I and MCo-PMI, residues 1 through 43. **F.** Changes in the  $\text{H-N}^\alpha$  protons and  $\text{N}^\alpha$  chemical shifts between Hdm2-bound and free MCo-PMI. **G.** Probability of secondary structure formation for the apamin-PMI grafted peptide segment on MCo-PMI (residues 36 through 50). The probabilities are based on the NH backbone chemical shifts ( $\text{H-N}^\alpha$  ( $\text{H}'$ ) and  $^{15}\text{N}$ ). The positive chemical shift index with respect to random coil implies that PMI loop is likely alpha helical.

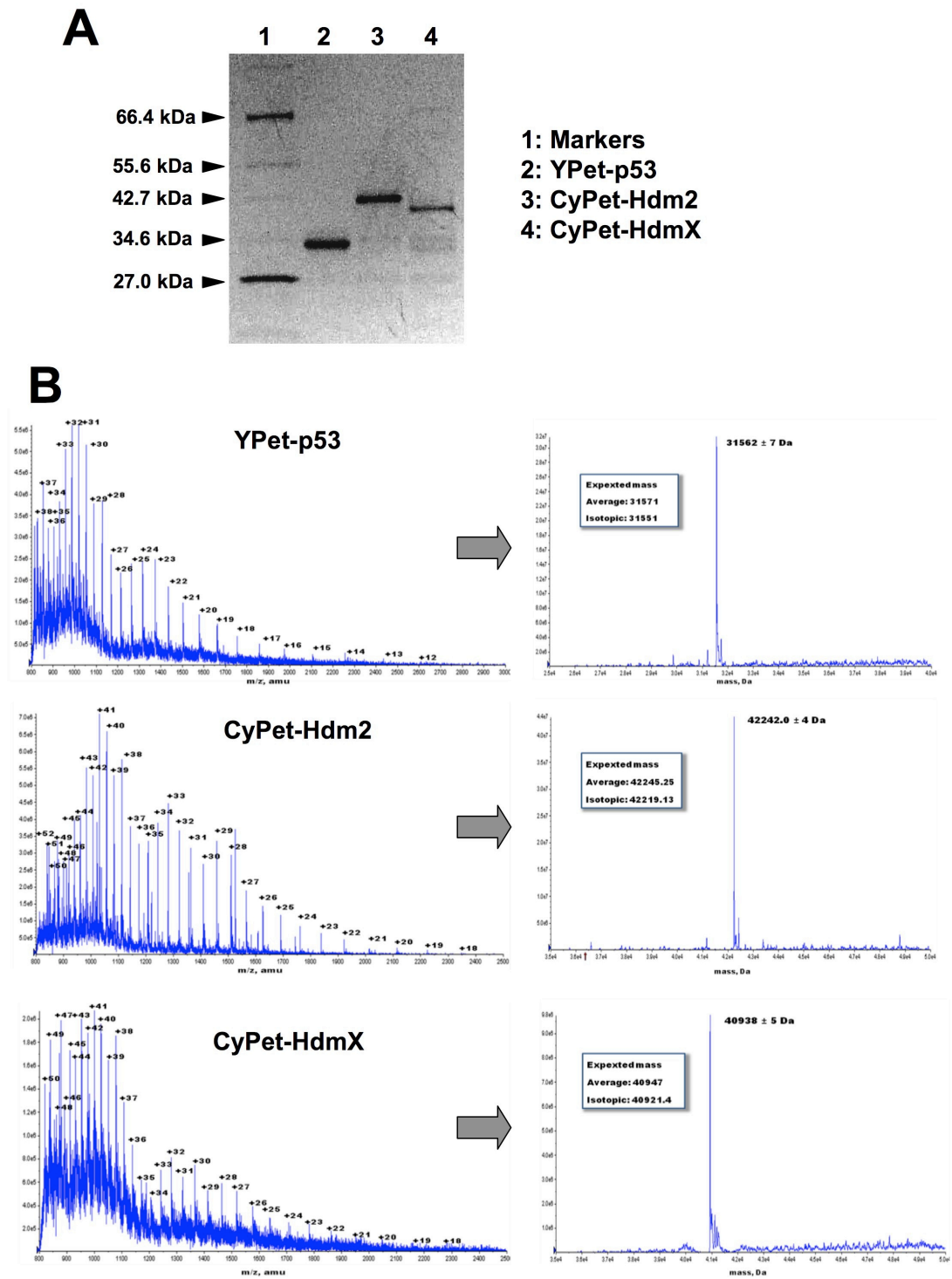


**Figure S4.** SDS-PAGE (A) and ES-MS spectra (B) of purified YPet-p53, CyPet-Hdm2 and CyPet-HdmX.

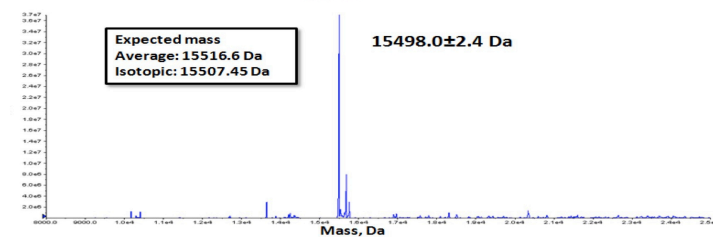
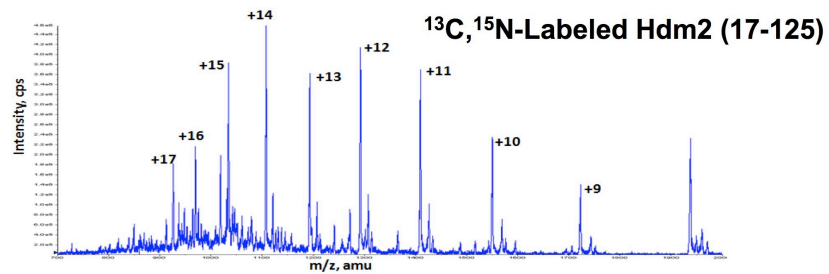
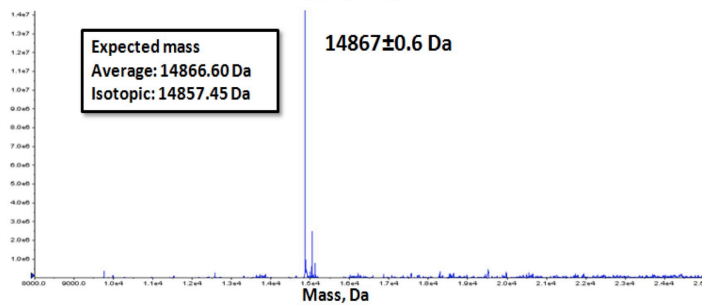
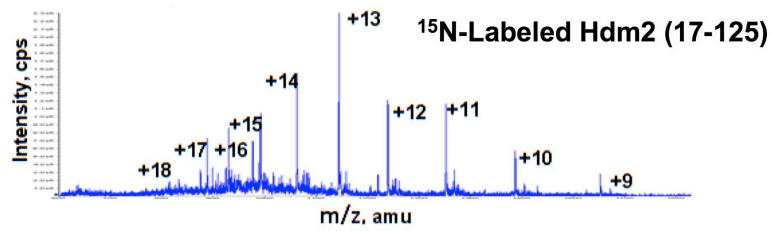


**Figure S5.** ES-MS spectra of <sup>15</sup>N- and <sup>13</sup>C, <sup>15</sup>N-labeled Hdm2 used for NMR spectroscopy.



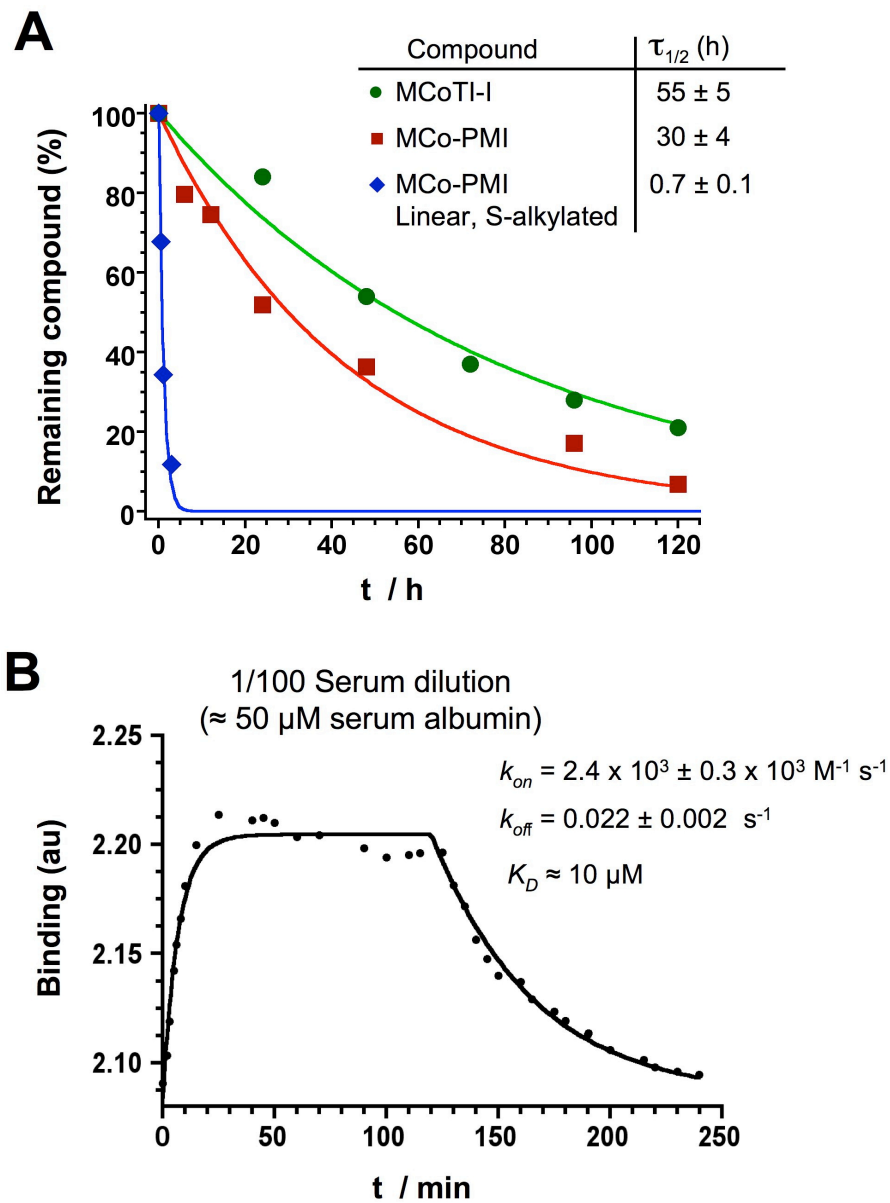


**Figure S6. A.** Serum stability of cyclotides MCo-PMI and MCoTI-I, and a linearized and S-alkylated version of MCo-PMI at 37°C. **B.** Binding kinetics of cyclotide MCo-PMI to human serum proteins.

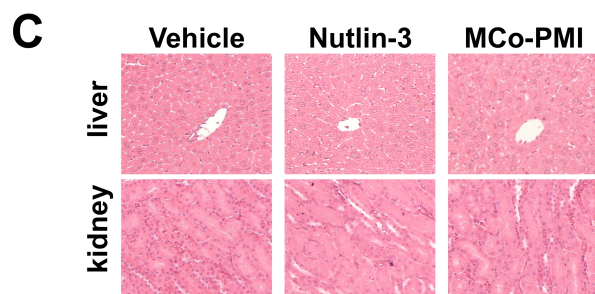
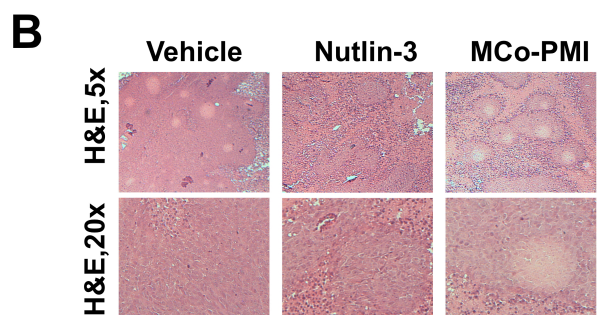
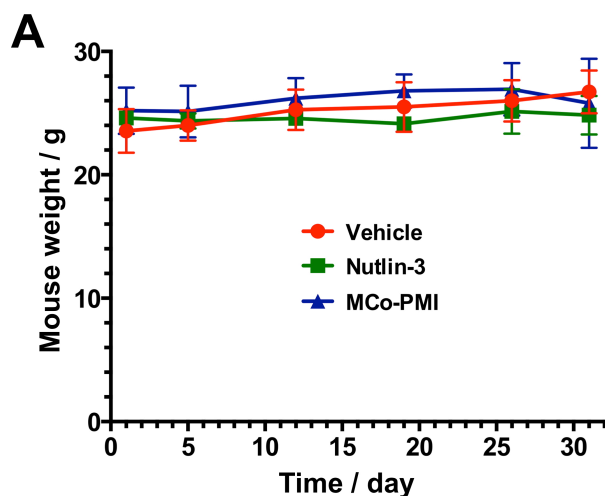


**Figure S7.** MCo-PMI treatment does not cause systemic toxicity. Cohorts (N = 3) of HCT116 p53<sup>+/+</sup> xenografts mice were treated with vehicle (D5W), MCo-PMI (40 mg/kg, 7.6 mmol/kg) or Nutlin-3 (10 mg/kg, 17.2 mmol/kg) daily for N days. **A.** Body weight was measured weekly using an electronic balance. Data are mean  $\pm$  SEM. No significant differences were noted between cohorts. Upon completion of treatment, tumors were excised and processed for histologic characterization. **B.** Micrographs showing histological features of H&E stained tumor sections at 5x and 20x magnifications, upper and lower panels, respectively. **C.** H&E stained sections of the kidney and liver, upper and lower panels, respectively.



## References

1. Kaduk, C., Wenschuh, H., Beyermann, M., Forner, K., Carpino, L. A., and Bienert, M. (1997) Synthesis of Fmoc-amino acid fluorides via DAST, an alternative fluorinating agent *Lett. Pept. Sci.* **2**, 285-288.
2. Ingenito, R., Dreznjak, D., Guffler, S., and Wenschuh, H. (2002) Efficient loading of sulfonamide safety-catch linkers by Fmoc amino acid fluorides, *Org. Lett.* **4**, 1187-1188.
3. Camarero, J. A., and Mitchell, A. R. (2005) Synthesis of proteins by native chemical ligation using Fmoc-based chemistry, *Protein Pept Lett* **12**, 723-728.
4. Contreras, J., Elnagar, A. Y., Hamm-Alvarez, S. F., and Camarero, J. A. (2011) Cellular uptake of cyclotide MCoTI-I follows multiple endocytic pathways, *J Control Release* **155**, 134-143.
5. Kimura, R. H., Steenblock, E. R., and Camarero, J. A. (2007) Development of a cell-based fluorescence resonance energy transfer reporter for Bacillus anthracis lethal factor protease, *Anal Biochem* **369**, 60-70.
6. Cavanagh, J., Fairbrother, W. J., Palmer, A. G., and Skelton, N. J. (1996) *Protein NMR Spectroscopy: Principles and practice*, Academic Press, San Diego.
7. Cavanagh, J., and Rance, M. (1992) Suppression of cross relaxation effects in TOCSY spectra via a modified DISI-2 mixing sequence., *J. Magn. Res.* **96**, 670-678.
8. Masse, J. E., and Keller, R. (2005) AutoLink: automated sequential resonance assignment of biopolymers from NMR data by relative-hypothesis-prioritization-based simulated logic, *J Magn Reson* **174**, 133-151.
9. Guntert, P. (2004) Automated NMR structure calculation with CYANA, *Methods Mol Biol* **278**, 353-378.
10. Cornilescu, G., Delaglio, F., and Bax, A. (1999) Protein backbone angle restraints from searching a database for chemical shift and sequence homology, *J Biomol NMR* **13**, 289-302.
11. Brooks, B. R., Brooks, C. L., 3rd, Mackerell, A. D., Jr., Nilsson, L., Petrella, R. J., Roux, B., Won, Y., Archontis, G., Bartels, C., Boresch, S., Caflisch, A., Caves, L., Cui, Q., Dinner, A. R., Feig, M., Fischer, S., Gao, J., Hodoscek, M., Im, W., Kuczera, K., Lazaridis, T., Ma, J., Ovchinnikov, V., Paci, E., Pastor, R. W., Post, C. B., Pu, J. Z., Schaefer, M., Tidor, B., Venable, R. M., Woodcock, H. L., Wu, X., Yang, W., York, D. M., and Karplus, M. (2009) CHARMM: the biomolecular simulation program, *Journal of computational chemistry* **30**, 1545-1614.
12. Laskowski, R. A., Rullmann, J. A., MacArthur, M. W., Kaptein, R., and Thornton, J. M. (1996) AQUA and PROCHECK-NMR: programs for checking the quality of protein structures solved by NMR, *J Biomol NMR* **8**, 477-486.
13. Zaro, J. L., and Shen, W. C. (2003) Quantitative comparison of membrane transduction and endocytosis of oligopeptides, *Biochem Biophys Res Commun* **307**, 241-247.